



Study of Non-linear Spectroscopic Optical Properties, Electrical Susceptibility and Semiconducting Dependence on Substrate Temperature for ZnO Thin Films Prepared by Radio Frequency Technique



Ahmed I. Ali^{1,2} and Ahmed Abdel Moez^{3*}

¹Basic Science Department, Faculty of Industrial Education, Helwan University, Kobry El-Qopa, Cairo, Egypt.

²Nanotechnology Research Center, The British University in Egypt, El Sherouk City, Suez Desert Road, Cairo 11837.

³Solid State Electronics Laboratory, Solid State Physics Department, Physics Research Division, National Research Centre (NRC), 33 El Bohouth St., Dokki, Giza, 12622, Egypt.

ZnO thin films which were prepared by radio frequency technique with different substrates temperature were investigated optically. The both of first linear optical susceptibility ($\chi^{(1)}$) and third order non-linear optical susceptibility ($\chi^{(3)}$) were determined. Moreover, other important non-linear optical parameters such as non-linear refractive index and non-linear absorption coefficient β_3 were determined for these studied samples. The electric susceptibility χ_e and relative permittivity ϵ_r for these samples were calculated optically. Finally, important semiconducting parameters such as density of valence band N_v , density of conduction band N_c , free carrier concentration ($N_d - N_a$), position of Fermi level E_f and surface electric field E_s were determined for these studied samples.

Keywords: ZnO thin films, RF sputtering, different substrate temperature, structure, first linear optical susceptibility, non-linear optical susceptibility, electrical susceptibility and semiconducting results.

Introduction

Recently Metal oxides have been attracted attentions as a result of their applications such as, gas sensors [1], surface acoustic devices [2], transparent electrodes [3], solar cells [4, 5], light emitting diodes [6], spintronic devices [7], nano-lasers [8] and Surface Acoustic Wave (SAW) device [9,10]. ZnO is an oxide semiconductor which has an electronic application such as photo-catalysts [11], thin film gas sensors [12], varistors [13] and other applications such as solar cell windows [14-16] and gas sensors [17-19]. Structural of ZnO Thin Films had been studied by many authors [20-22], it was found that, ZnO samples have hexagonal structure [23-25].

ZnO thin films have a good non-linear second-order susceptibility [26-28]. The study of third-harmonic generation in thin nanocrystalline ZnO near-IR radiation has studied [29]. The second-harmonic generation theory of ZnO samples had investigated [30-34]. The non-linearity on at different conditions [35] and two-photon resonance [36], doping effect on non-linear susceptibility were studied [37-38]. The nondegenerate non-linear absorption coefficient for ZnO using pairs of extremely nondegenerate photons was investigated [39]. On the other hand, the influence of substrate temperature physical of ZnO thin films were studied [40-42], it was found that, the energy gap decreased with substrate temperature [40].

*Corresponding author e-mail: aam692003@yahoo.com; Phone: +2(0115)4764607

Received 28/2/2019; Accepted 10/6/2019

DOI: 10.21608/EJCHEM.2019.12748.1792

© 2019 National Information and Documentation Center (NIDOC)

Experimental work

ZnO thin films were prepared using Radio Frequency (RF) technique. These films were prepared under vacuum less than 5.0×10^{-6} Torr, onto quartz substrates which were placed into RF sputtering, these films were prepared using ZnO ingot powder of purity (99.99 %). The powder was placed in a disc target of four inches diameter. RF sputtering was adjusted with a power of 150 W for one hour with different substrate temperatures (room temperature, 100, 200, 300, 400 and 500°C). The distance between the powder target and the substrate was maintained at 10 cm. Ar gas with a purity of 99.999% with a rate of flow 30 cm³/min was injected during sputtering process.

The microstructures of the ZnO films were investigated using scanning electron microscopy

(SEM; JEOL, JSM6335F) and X-ray diffraction (XRD; Rigaku, D/MAX-Rc) with Cu K_α radiation at a wavelength of 1.54 Å. The transmission spectra of the films were measured using UV/VIS double-beam spectrophotometer (Cary 5E) with a wavelength range from 300 nm to 800 nm.

Results and Discussion

Structure

The surface structure for the ZnO thin films with different substrates temperatures is shown in Fig. 1. From this Fig. it was seen that, the grain size of increase with substrate temperature. While surface topography using Atomic Force Microscope (AFM). The X-ray results of these studied samples was carried out in our previous work [40].

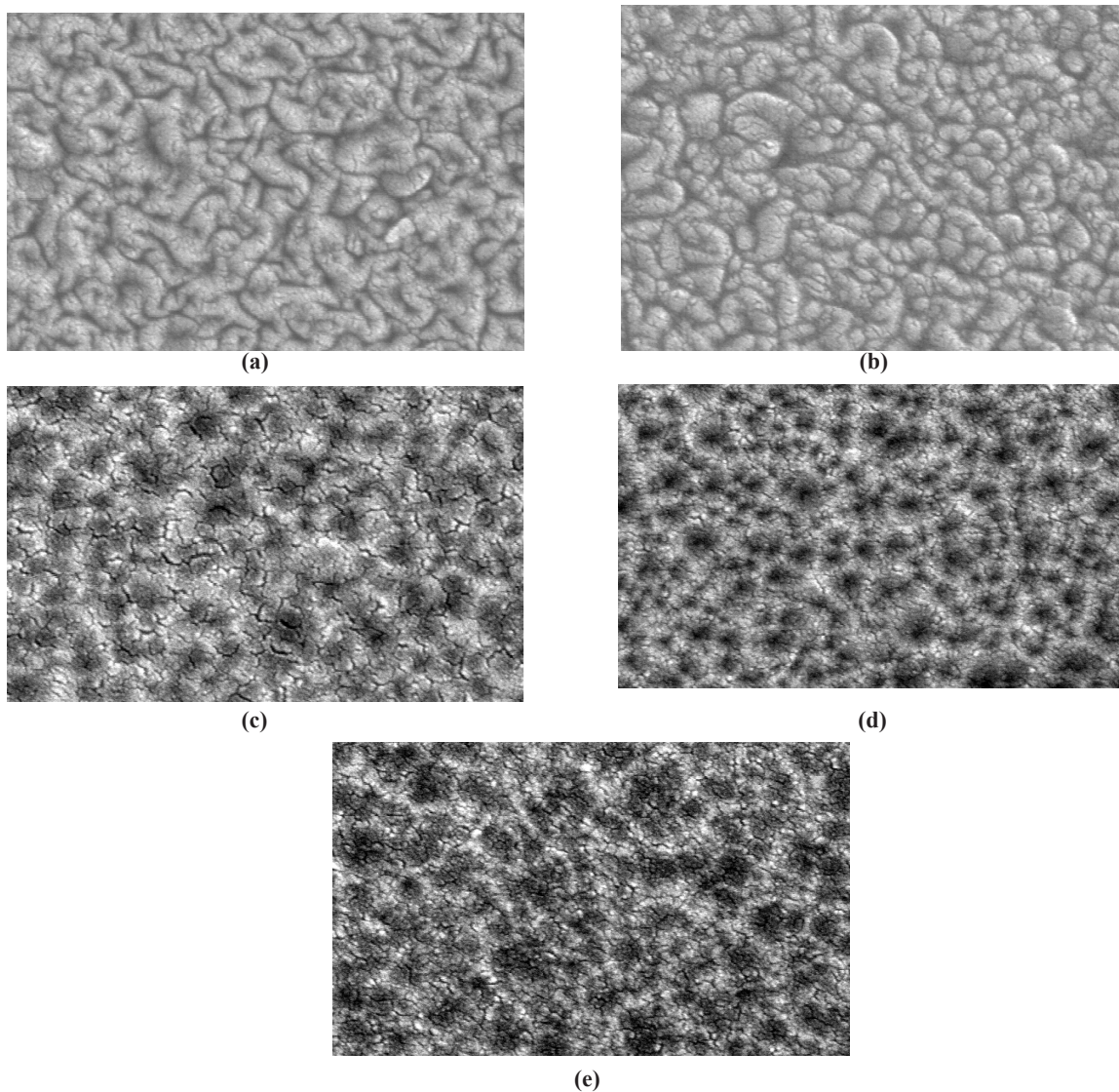


Fig. 1. Scanning electron Microscope (SEM) picture for ZnO thin films with different substrate temperature (a) 100, (b) 200, (c)300, (d) 400 and (e) 500 °C.

Non-linear optical results

The third-order non-linear optical susceptibility $\chi^{(3)}$ was determined using the following formula [43]:

$$\chi^{(3)} = A \left[\frac{E_o \cdot E_d}{4\pi(E_o^2 - (h\nu)^2)} \right]^4 \quad (1)$$

where A is 1.7×10^{-10} e.s.u [43], E_o is the oscillator energy and E_d is the dispersion energy for these studied samples and had been determined in our previous work [40].

The dependence of $\chi^{(3)}$ on wave length (λ) for these samples is shown in Fig. 2. From this Fig. it is seen that, $\chi^{(3)}$ increase with photon energy ($h\nu$) for all these studied samples. This could be due to, when ($h\nu$) increases, the deflection of the incident light beam increases. While $\chi^{(3)}$ increased with substrate temperature, due to when substrate temperature increases, the conductivity of these samples increase as a result of increasing the mobility of electron .

On the other hand, the both of real and imaginary part $\chi^{(3)}$ was determined using the following equations [44]

$$\text{Re } \chi^{(3)} = 10^{-4} \left(\frac{\epsilon_o n_o^2 c^2}{\pi} \right) n_2 \quad (2)$$

$$\text{Im } \chi^{(3)} = 10^{-2} \left(\frac{\epsilon_o n_o^2 c^2}{4\pi^2} \right) \beta_o \quad (3)$$

Where ϵ_o is Vacuum permittivity $\epsilon_o = 8.854187817 \times 10^{-12}$ F.m⁻¹ [45], β_o is the non-linear absorption coefficient, c is the speed of light, n_o is the static refractive index and n_2 is the non-linear refractive index.

The relation between ($h\nu$) and both of the $\text{Re } \chi^{(3)}$ and $\text{Im } \chi^{(3)}$, for these samples are shown in Fig. 3 and 4. Respectively. From this Fig it was noticed that, $\text{Re } \chi^{(3)}$ and $\text{Im } \chi^{(3)}$ increase with ($h\nu$) for all these studied samples, this could be attributed to, when the ($h\nu$) increases this leads to increase of excited electrons which increase of $\chi^{(3)}$.

An important parameter of the non-linear optical parameters is that the non-linear refractive index (n_2), which was determined from the following simple equation [46-47].

$$n_2 = \left(\frac{12\pi\chi^{(3)}}{n_o} \right)^{0.5} \quad (4)$$

Where (n_o) is static refractive index, which was determined for these studied samples using the following Equation. [48]

$$n_o = \left(\frac{E_d}{E_o} + 1 \right)^{0.5} \quad (5)$$

The values of (n_o) for all studied samples is shown in Table 1. n_o increased with substrate temperature, as result of increase both value of E_o , E_d with substrate temperature, as shown in Table 1. The dependence of the determined non-linear refractive index (n_2) on (λ) is shown in Fig. 5, as it is clear from this Fig. (n_2) increases with substrate temperature, this is because of increasing grain size with substrate temperature, as shown in Fig. 1.

The non-linear absorption coefficient (β_o) which is the different frequencies in order to excite a molecule from one to a higher energy electronic state, and was determined using the following equation [49]:

$$\beta_o = \left(\frac{38\pi^3 \chi^{(3)}}{c\lambda n^2} \right) \quad (6)$$

Where n is the refractive index which had been calculated for these samples in our previous work [40].

The dependence of (β_o) on ($h\nu$) for ZnO thin films is illustrated in Fig.6, from this Fig. it shown that, the behavior of the (β_o) increased for all these samples with ($h\nu$), this could be attributed to, when ($h\nu$) increases the number of excited electrons increases, which cause an increase of (β_o).

Linear optical susceptibility

linear optical susceptibility $\chi^{(1)}$ describes the response of the material to an optical wave length and was determined using the following relation [50]:

$$\chi^{(1)} = \frac{(n^2 - 1)}{4\pi} \quad (7)$$

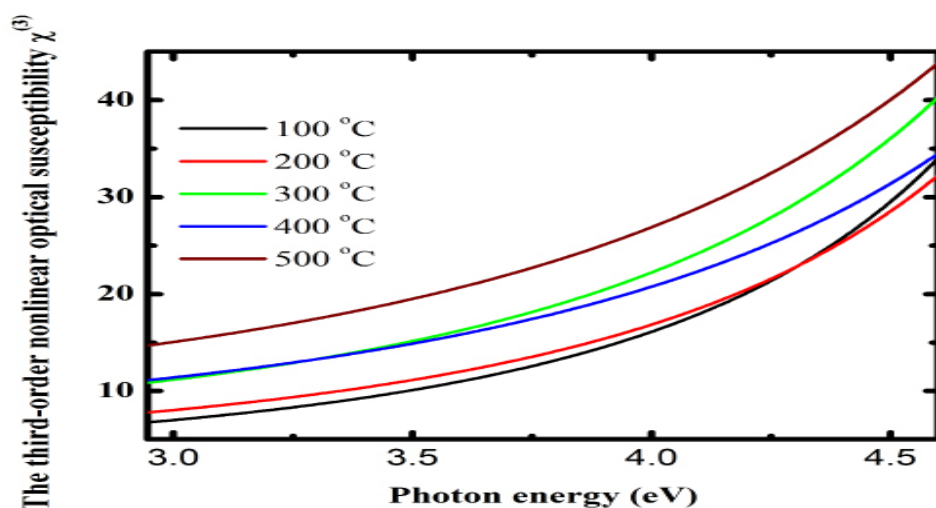


Fig. 2. The third-order non-linear optical susceptibility $\chi^{(3)}$ dependence on photon energy for ZnO thin films with different substrate temperature (a) 100, (b) 200, (c)300, (d) 400 and (e) 500°C.

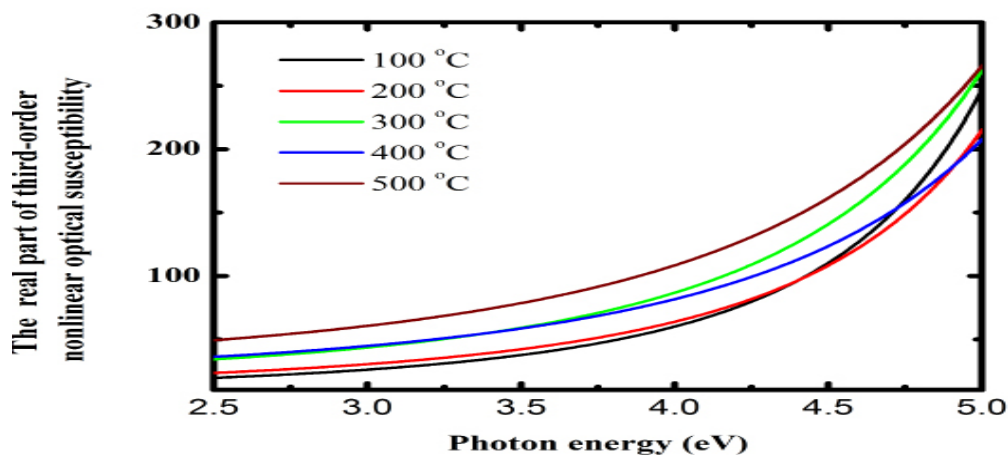


Fig. 3. Relation between the real part of third-order non-linear optical susceptibility and photon energy for ZnO thin films with different substrate temperature (a) 100, (b) 200, (c)300, (d) 400 and (e) 500°C.

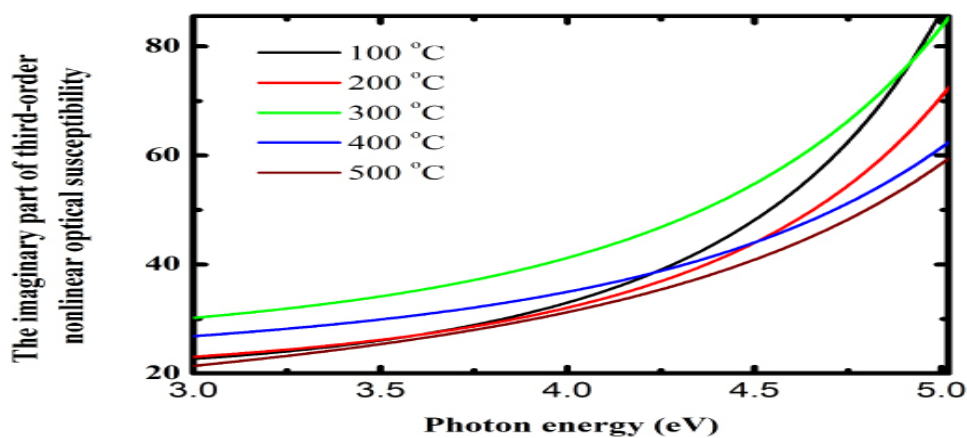


Fig. 4. Relation between the imaginary part of third-order non-linear optical susceptibility and photon energy for ZnO thin films with different substrate temperature (a) 100, (b) 200, (c)300, (d) 400 and (e) 500°C.

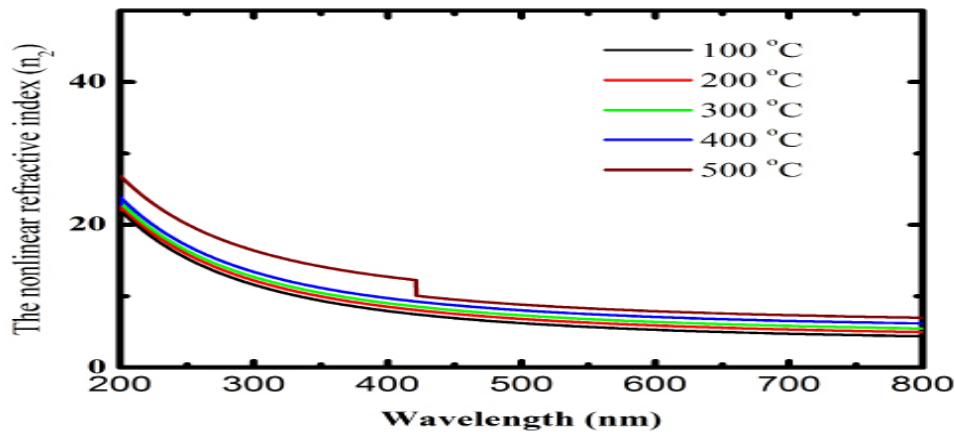


Fig. 5. The non-linear refractive index dependence on wave length for ZnO thin films with different substrate temperature (a) 100, (b) 200, (c)300, (d) 400 and (e) 500 °C.

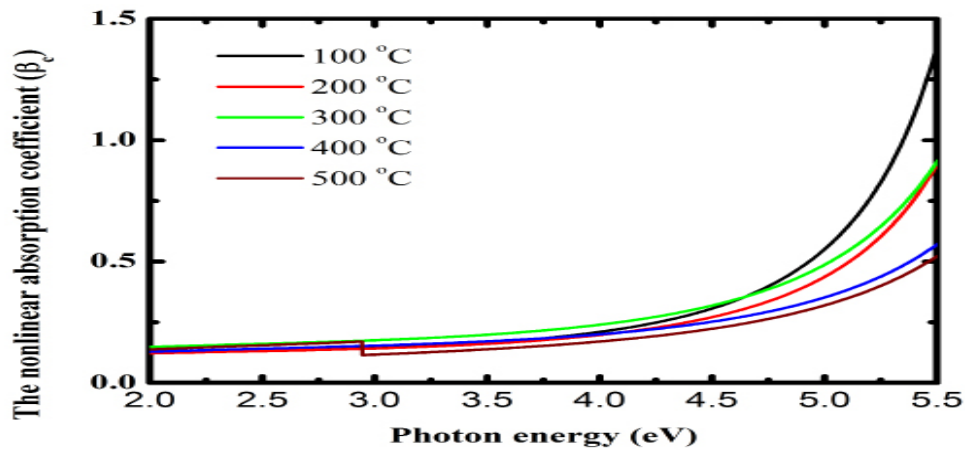


Fig. 6. The non-linear absorption coefficient (β) dependence on photon energy for ZnO thin films with different substrate temperature (a) 100, (b) 200, (c)300, (d) 400 and (e) 500 °C.

TABLE 1. The determined values of ZnO thin films such as static refractive index (n_0), Free carrier concentration N_d-N_a (cm^{-3}), density of conduction band N_c (cm^{-3}), density of valence band N_v (cm^{-3}) and Fermi level position (eV) and Surface electric E_s (kV).

Temperature °C	Oscillator energy E_o (eV) [38]	Dispersion energy E_d (eV) [38]	N/m^* [38]	Static refractive index (n_0)	N_c (cm^{-3})	N_v (cm^{-3})	Fermi level position (eV)	N_d-N_a (cm^{-3})	Surface electric E_s field (kV)
100	6.80	9.80	1.1E+48	1.56	7.42E+20	3.30E+20	1.16	2.64E+20	46.20
200	7.10	10.80	1.2E+48	1.59	2.10E+21	9.32E+20	1.00	2.88E+20	50.30
300	7.30	12.20	9.7E+47	1.63	3.85E+21	1.71E+21	0.84	2.33E+20	40.70
400	7.70	13.20	8.3E+47	1.65	5.93E+21	2.64E+21	0.80	1.99E+20	34.80
500	7.80	14.40	8.3E+47	1.69	8.29E+21	3.68E+21	0.78	1.99E+20	34.80

The relation between $\chi^{(1)}$ and $(h\nu)$ for ZnO thin films with different substrate temperature is shown in Fig. 7. From this Fig. it was seen that, $\chi^{(1)}$ increased for all these samples with $(h\nu)$, this due to, the increase when $(h\nu)$ increases, the incident light intensity, increases which cause an increase $\chi^{(1)}$.

Electrical Susceptibility

Electrical susceptibility $\chi_{(e)}$, which describe the electrical behavior of the samples under the influence of the electric field and was determined using the following relation [51]

$$\chi_{(e)} = \frac{(n^2 - k^2 - \epsilon_o)}{4\pi} \quad (8)$$

Where k is the extinction coefficient which was calculated for these samples in our previous work [40].

The dependence of $\chi_{(e)}$ on $(h\nu)$ of these investigated samples is shown in Fig. 8. From this Fig. it is clear that the values of $\chi_{(e)}$ for all these samples increase with $(h\nu)$. This could be attributed to the increase of electron mobility with $(h\nu)$, which leads to the increase of the electric susceptibility $\chi_{(e)}$.

The relative permittivity ϵ_r was calculated using the following relation [52]

$$\epsilon_r = (\chi_e + 1) \quad (9)$$

The relation between ϵ_r and (λ) for these films is shown in Fig. 9. From this Fig. it was seen that, the values of relative permittivity ϵ_r increases with $(h\nu)$ for all these samples, this could be attributed to the increase of relative permittivity ϵ_r is due to the increase of the electrical susceptibility.

Semiconducting Results

The semiconducting results plays an important role for changing both of electrical and optical properties, so it is important for explanation of the physical properties is that, determination of these semiconducting parameters.

The density of state for both the valence and conduction band were calculated using the following equations [53]:

$$Ef = \frac{KT}{q} \cdot \ln\left(\frac{N_c}{N_v}\right) \quad (10)$$

Where N_v , N_c were the density of states for both valence and conduction bands respectively, m_e^* is the effective mass of electrons and had a value of $0.24 m_o$ [54], m_h^* is the effective mass of holes and had a value of $0.45 m_o$ [55], K is the Boltzmann constant and T is the temperature on Kelvin.

The determined values of both N_v , N_c are shown in Table 1. The most important factor was determined as a function of N_v , N_c , this is the position of Fermi level, which was determined using the following relation [53].

The determined values of the Fermi level Position (FLP) from conduction band is shown in Table 1, which showed that the values of (FLP) decreases with substrate temperature.

The determined free carrier concentration gives an indication of an important semiconducting parameter which is, surface electric field (E_s), which was determined using the following relation

$$E_s = \left[\frac{2e \cdot [N_d - N_a] (V_s - kT/e)}{\epsilon \epsilon_0} \right] \quad (11)$$

Where e is the electron charge, $(N_d - N_a)$ is the calculated free carrier concentration, ϵ dielectric permittivity of ZnO and had a value of 2.08 [56]

And V_s is the pinning of Fermi level and equal 0.66 eV [57]. The determined values of the surface electric field is shown in Table .1, which showed that, the surface electric field decreases with substrate temperature, this is due, the electron mobility increases when the substrate temperature increase, which increase the electron hole recombination at the surface of the sample, which leads finally to decreased the surface electric field.

Conclusion

The high-quality thin films of ZnO were prepared with different substrate temperature deposition (100–500 C) using RF method. The SEM

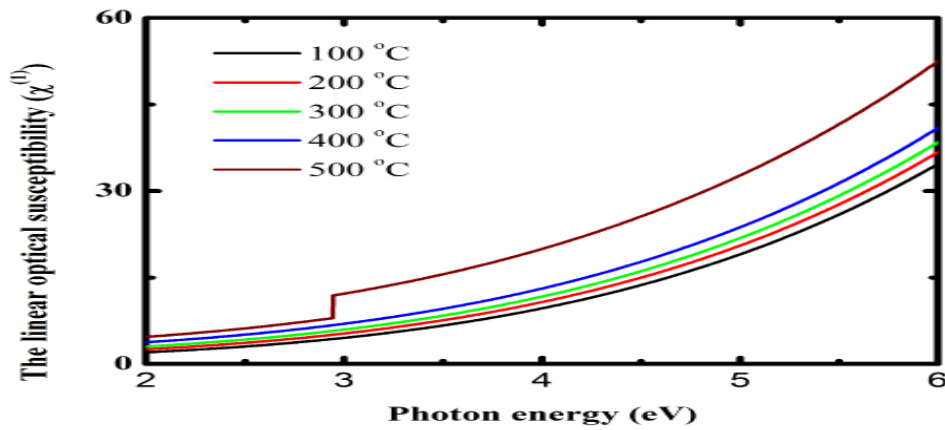


Fig. 7. The linear optical susceptibility $\chi^{(1)}$ dependence on photon energy for ZnO thin films with different substrate temperature (a) 100, (b) 200, (c)300, (d) 400 and (e) 500 oC.

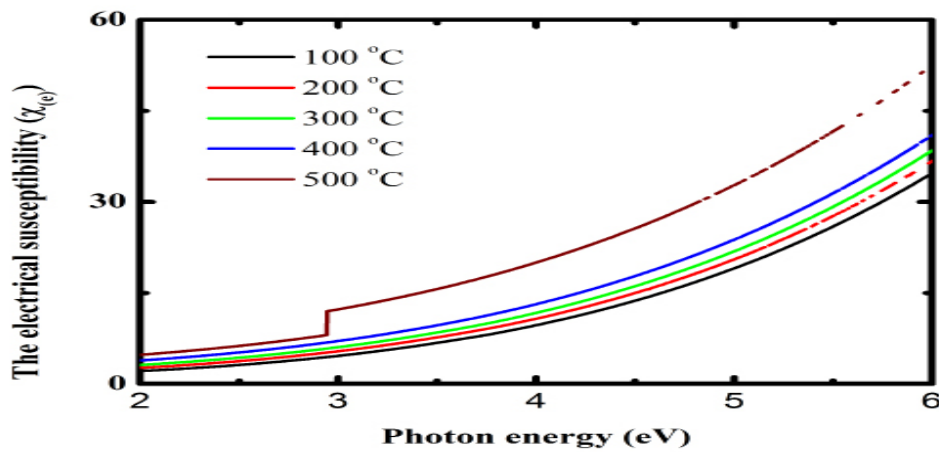


Fig. 8. Relation between the electrical susceptibility $\chi_{(e)}$ and photon energy for ZnO thin films with different substrate temperature (a) 100, (b) 200, (c)300, (d) 400 and (e) 500 °C.

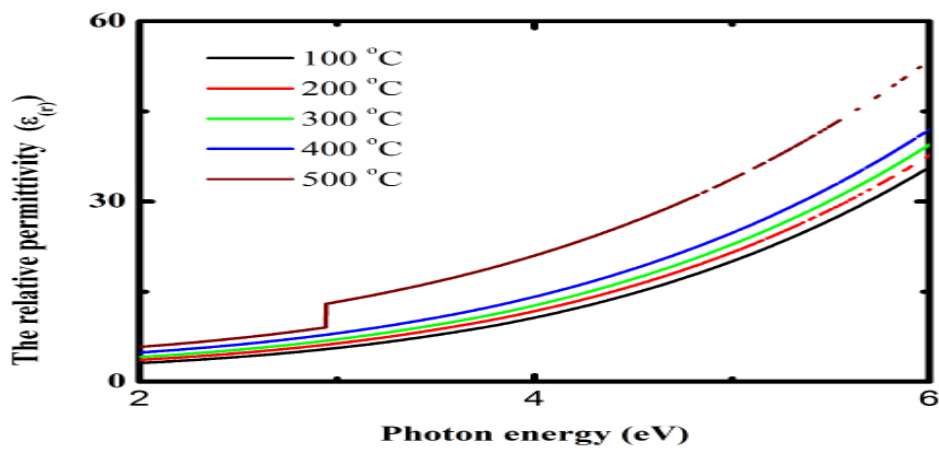


Fig. 9. Relation between relative permittivity ϵ_r and photon energy for ZnO thin films with different substrate temperature (a) 100, (b) 200, (c)300, (d) 400 and (e) 500 °C.

pictures showed that, the grain size increased with substrate temperature. The values of $\chi^{(3)}$ increase with $(h\nu)$ for all samples as a result of increased the mobility of electron increased, both of the real and imaginary part of $\chi^{(3)}$ increased with $(h\nu)$ for these samples for all substrate temperatures. The values of the n_2 for all these studied samples decreased with (λ) , this is due to the increasing of grain size with substrate temperature. (β_c) increased for all these samples with $(h\nu)$, which is due to, $(h\nu)$ increase the number of excited electrons. The same behavior was noticed for $\chi^{(1)}$ Which increased with $(h\nu)$ as a result of increase of incident light intensity, also both of electrical susceptibility χ_e and relative permittivity ϵ_r increase with $(h\nu)$ as a result of the electron mobility increases with $(h\nu)$. The values of both N_v , N_c increased with substrate temperature. This is due to the increase in the electron and hole motilities. On the other hand, the determined values of both of (FLP) and E_s decrease with substrate temperature as a result of increasing the electron hole recombination at the surface of the sample with substrate temperature. These results give a great chance for control and change the important results such as structure, non-linear optical results and semiconducting results.

By changing the substrate temperature of deposition only, this leads to important industrial applications such as electronic and optoelectronic devices with low cost.

References

1. Suche M., Christoulakis S., Moschovis K., Katsarakis N. and Kiriakidis G., ZnO transparent thin films for gas sensor applications, *Thin Solid Films*, **515**, 551-554 (2006).
2. Water W., Chu S.Y., Juang Y.D. and Wu S.J., Li_2CO_3 -doped ZnO films prepared by RF magnetron sputtering technique for acoustic device application, *Mater. Lett.*, **57**, 998-1003 (2002).
3. Michelotti F., Belardini A., Rousseau A., Ratsimihety A., Schoer G. and Mueller J., Use of sandwich structures with ZnO:Al transparent electrodes for the measurement of the electro-optic properties of standard and fluorinated poled copolymers at $\lambda = 1.55 \mu\text{m}$, *J. Non-Cryst. Solids*, **352**, 2339-2342 (2006).
4. Hupkes J., Rech B., Kluth O., Repmann T., Zwaygardt B., Muller J., Drese R. and Wuttig M., The Preparation and Properties of Al-Doped ZnO Thin Films as Transparent Electrodes for Solar Cell, *Sol. Energ. Mat. Sol. C*, **90**, 3054-3060 (2006).
5. Jeong W.J., Kim, S.K. and Park G.C., Preparation and characteristic of ZnO thin film with high and low resistivity for an application of solar cell, *Thin Solid Films*, **506-507**, 180-183 (2006).
6. Saito N., Haneda H., Sekiguchi T., Ohashi N., Sakagu-chi I. and Koumoto K., Low-Temperature Fabrication of Light-Emitting Zinc Oxide Micropatterns Using Self-Assembled Monolayers, *Adv. Mater.*, **14**(6), 418-421 (2002).
7. Meron T. and Markovich G., Ferromagnetism in Colloidal Mn^{2+} -Doped ZnO Nanocrystals, *J. Phys. Chem. B*, **109**, 20232- 20236 (2005).
8. Huang M.H., Mao S., Feick H., Yan H., Wu Y., Kind H., Weber E., Russo R. and Yang, P., Room temperature Ultraviolet nanowire nanolasers, *Science*, **292**, 1897-1899 (2001).
9. Webb J.B., Williams D.F., Buchanan M., Transparent and highly conductive films of ZnO prepared by RF reactive magnetron sputtering, *Appl. Phys. Lett.*, **39**, 640-642 (1981).
10. Kang S.J., Choi J.Y., Chang D.H. and Yoon Y.S., A Study on the Growth and Piezoelectric Characteristics of ZnO Thin Film Using a RF Magnetron Sputtering Method, *Journal of Korean Physical Society*, **47**, S589-S594 (2005).
11. Chakrabarti S. and Dutta B.K., Photocatalytic Degradation of Model Textile Dyes in Wastewater Using ZnO as Semiconductor Catalyst. *J. Hazard. Mater.*, **112**, 269-278 (2004).
12. Shishiyanu S.T., Shishiyanu T.S. and Lupen O.I., Sensing Characteristics of Tin-Doped ZnO Thin Films as NO_2 Gas Sensor, *Sensor. Actuat. B-Chem*, **107**, 379-386 (2005).
13. Ammar A.H. and Farag A.A.M., Investigation of deep level transient spectroscopy (DLTS) of dopant ZnO-based varistors, *Physica B*, **405**, 1518-1522 (2010).
14. Yang T.L., Zhang D.H., Ma J., Ma H.L. and Chen Y., Transparent conducting ZnO:Al films deposited on organic substrates deposited by r.f. magnetron-sputtering, *Thin Solid Films*, **326**, 60-62 (1998).
15. Francombe M.H. and Krishnaswamy S.V., Growth and properties of piezoelectric and ferroelectric films. *J. Vac. Sci. Technol. A*, **8**, 1382-1391 (1990).

16. Sang B., Yamada A. and Konagai M., Textured ZnO Thin Films for Solar Cells Grown by a Two-step Process with the Atomic Layer Deposition Technique, *Jpn. J. Appl. Phys.*, **37**, L206-09 (1998).
17. Calestani D., Zha M., Mosca R., Zappettini A., Carotta M.C., Di Natale V. and Zanotti L., Growth of ZnO tetrapods for nanostructure-based gas sensors, *Sensor. Actuat. B-Chem.*, **144**, 472-478 (2010).
18. Gupta S. K., Joshi A. and Kaur M., Development of gas sensors using ZnO nanostructures, *J. Chem. Sci.*, **122**, 57-62 (2010).
19. Liu F.T., Gao S.F., Pei S.K., Tseng S.C. and Liu C.H.J., ZnO nanorod gas sensor for NO₂ detection, *J. Taiwan Inst. Chem. E.*, **40**, 528-532 (2009).
20. Bahadur H., Srivastava A.K., Haranath D., Chander H., Basu A., Samanta S.B., Sood K.N., Kishore R., Sharma R., Rashmi K., Bhatt V., Pal P. and Chandra S., NanoStructured ZnO Films by Sol-Gel Process, *Indian Journal of Pure and Applied Physics*, **45**, 395-399 (2007).
21. Li H.X., Wang J.Y., Liu H., Zhang H.J. and Li X., Zinc Oxide Films Prepared by Sol-Gel Method, *J. Cryst. Growth*, **275**, e943-946 (2005).
22. Khan Z.R., Khan M.S., Zulfequar M. and Khan M.S., Optical and Structural Properties of ZnO Thin Films Fabricated by Sol-Gel Method, *Materials Sciences and Applications*, **2**, 340-345 (2011).
23. Alias M.F.A., Aljarrah R.M., Al-Lamy H.K.H. and Adem K.A.W., Investigation the Effect of Thickness on the Structural and Optical Properties of Nano ZnO Films Prepared by d.c Magnetron Sputtering, *International Journal of Application or Innovation in Engineering & Management*, **2**, 198-203 (2013).
24. Asmaa S.M., El Nagger A.M.A., Sahar M.T., Omar I., Sana I.H. and Ahmed I.H., Preparation and Characterization of MicroPorous ZnO Nanoparticles, *Egypt. J. Chem.*, **59**, 609- 621 (2016).
25. Hanna A.A., Mohamed W.A.A. and Hoda R.G., Preparation, Characterization and Evaluation of Nano Zinc Oxides as Pigments. *Egypt. J. Chem.*, **57**, 423- 433 (2014).
26. Newmann, U., Grunwald, R., Griedner, U., and Steinmeyer, G. Second-harmonic efficiency of ZnO nanolayers, *Appl. Phys. Lett.*, **84**, 170-173 (2004).
27. Wang G., Kiehne G.T., Wong G.K.L., Ketterson J.B., Liu X. and Chang R.P.H., Large second harmonic response in ZnO thin films, *Appl. Phys. Lett.*, **80**, 401-404 (2002).
28. Irimpan L., Krishnan B., Deepthy A., Nampoori V.P.N. and Radhakrishnan P., Size-dependent enhancement of non-linear optical properties in nanocolloids of ZnO, *J. Appl. Phys.*, **103**, 33105-33106 (2008).
29. Petrov G.I., Shcheslavskiy V., Yakovlev V.V., Ozerov I., Cheinokov E. and Marine W., Efficient third-harmonic generation in a thin nanocrystalline film of ZnO, *Appl. Phys. Lett.*, **83**, 3993-3996 (2003).
30. Lin J.H., Chen Y.J., Lin H.Y. and Hsieh W.F., Two-photon resonance assisted huge non-linear refraction and absorption in ZnO thin films, *J. Appl. Phys.*, **97**, 033526-33527 (2005).
31. Wang, G., Kiehne G.T., Wong G.K.L., Ketterson J.B., Liu Z. and Chang R.P.H., Large second harmonic response in ZnO thin films, *Appl. Phys. Lett.*, **80**, (2002) 401-404.
32. Han N.S., Shim H.S., Park S.M. and Song J.K., Second-harmonic Generation and Multiphoton Induced Photoluminescence in ZnO, *B. Korean Chem. Soc.*, **30**, 2199-2201 (2009).
33. Zhang C.F., Dong Z.W., You G.J., Zhu R.Y., Qian S.X., Deng H., Cheng H. and Wang J.C., Femtosecond pulse excited two-photon photoluminescence and second harmonic generation in ZnO nanowires, *Appl. Phys. Lett.*, **89**, 042117 (2006).
34. Lo K.Y. and Huang Y.J., Reflective second harmonic generation from ZnO thin films: A study on the Zn-O bonding, *Appl. Phys. Lett.*, **90**, 161904-161905 (2007).
35. Han Y.B., Han J.B., Ding S., Chen D.J. and Wang Q.Q., Optical non-linearity of ZnO microcrystallite enhanced by interfacial state, *Opt. Express*, **13**, (2005) 9211-9216.
36. Pei Chan Y., Lin J.H., Hsu C.C. and Hsieh W.F., Near-resonant high order non-linear absorption of ZnO thin films, *Opt. Express*, **16**, 19900-19908 (2008).
37. Teng Y., Ying L., Jun-Jie K., Peng-Yu Z., Quan S.B., Kun Z., Shen Y.S. and Hui Z.X., The Third-Order Non-linear Optical Properties in Cobalt-Doped ZnO Films, *Chinese Phys. Lett.*, **32**, 077801-077802 (2015).

38. Kavitha M.K., Haripadmam P.C., Gopinath P., Krishnan B. and John H., Effect of morphology and solvent on two-photon absorption of nano zinc oxide, *Mater. Res. Bull.*, **48**, 1967-1971 (2013).
39. Cirloganu C.M., Padilha L.A., Fishman D.A., Webster S., Hagan D.J. and Van Stryland E.W., Extremely nondegenerate two-photon absorption direct-gap Semiconductors, *Opt. Express*, **19**, 22951-22960 (2011).
40. Ali A.I., Ammar A.H. and Abdel Moez A., Influence of substrate temperature on structural, optical properties and dielectric results of nano- ZnO thin films prepared by Radio Frequency technique, *Superlattice Microst.*, **65**, 285-298 (2014).
41. Nabeel A.B., Ziad T.K. and Adnan M.S., Temperature on Structural and Optical Properties of ZnO Thin Films Prepared by APCVD Technique, *International Journal of Applied Engineering Research*, **13**, 10796-10803 (2018).
42. Georgi M., Velichka S., Marina V., Violeta M., Nikola M. and Tsvetanka B., Effect of Substrate Temperature on the Microstructural, Morphological, and Optical Properties of Electrospayed ZnO Thin Films, *Adv. Cond. Matter Phys.*, **2018**, 1-7 (2018).
43. Ziabari A.A. and Ghodsi F.E., Optoelectronic studies of sol-gel derived nanostructured CdO-ZnO composite films, *J. Alloy. Compd.*, **509**, 8748-8755 (2011).
44. Mathews S.J., Kumar C.S., Giribabu L. and Rao S.V., Large third-order optical non-linearity and optical limiting in symmetric and unsymmetrical phthalocyanines studied using Z-scan, *Opt. Commun.*, **280**, 206-212 (2007).
45. CODATA Value: electric constant. The NIST Reference on Constants, Units, and Uncertainty. US National Institute of Standards and Technology (2015). Retrieved 2015-09-25.
46. Tichá H. and Tichy L., Semiempirical relation between non-linear susceptibility (refractive index), linear refractive index and optical gap and its application to amorphous chalcogenides, *J. Optoelectron. Adv. M.*, **4**(2), 381-386 (2002).
47. Zhou P., You G., Li J., Wang S., Qian S. and Chen L., Annealing effect of linear and non-linear optical properties of Ag:Bi₂O₃ nanocomposite films, *Opt. Express*, **13**, 1508-1514 (2005).
48. Anshu K. and Sharma A., Study of Se based quaternary Se Pb (Bi,Te) chalcogenide thin films for their linear and non-linear optical Properties, *Optik*, **127**, 48-54 (2016).
49. Derkowska B., Sahraoui B., Phu X.N. and Bala W., Non-linear optical properties in ZnSe crystals. *Proceedings of SPIE*, **4412**, 337-341 (2001).
50. Fritz S.E., Kelley T.W. and Frisbie C.D., Effect of Dielectric Roughness on Performance of Pentacene TFTs and Restoration of Performance with a Polymeric Smoothing Layer, *J. Phys. Chem. B*, **109**, 10574-10577 (2005).
51. Gupta V. and Mansingh A.I., Influence of post deposition annealing on the structural and optical properties of sputtered zinc oxide film, *J. Appl. Phys.*, **80**, 1063-1074 (1996).
52. Braslavsky S.E., Glossary of terms used in Photochemistry, *Pure Appl. Chem.*, **79**, 293-465 (2006).
53. Sze S.M., Physics of Semiconductor Devices, Wiley-Inter science, New York (1969).
54. Oshikiri M., Imanaka Y., Aryasetiawan F. and Kido G., Comparison of the electron effective mass of the n-type ZnO in the wurtzite structure measured by cyclotron resonance and calculated from first principle theory, *Physica B*, **298**, 472-476 (2001).
55. Lambrecht W.R.L., Rodina A.V., Limpijumnonng S., Segall B. and Meyer B.K., Valence-band ordering and magneto-optic exciton fine structure in ZnO, *Phys. Rev. B*, **65**, 075207-075208 (2002).
56. Ma Ai.Y., Zhang L.B., Peng J.H., Chen G., Hui C.L., Xia H.Y. and Zuo Y.G., Dielectric Properties and Temperature Increase of Zinc Oxide Dust Derived from Volatilization in Rotary Kilns, *J. Microwave Power EE.*, **48**, 25-34 (2014).
57. Sabitova A., Ebert Ph., Lenz A., Schaafhausen S., Ivanova L., Dahne M., Hoffmann A., Dunin-Borkowski R.E., Forster A., Grandidier B. and Eisele H., Intrinsic band gap of cleaved ZnO (1120) surfaces, *Appl. Phys. Lett.*, **102**, 021608-0221609 (2013).

دراسة اعتماد الخواص البصرية الطيفية غير الخطية والقابلية الكهربائية و خواص شبه الموصلة على تغيير درجة حرارة قاعدة الترسيب لاغشية رقيقة من اكسيد الزنك المحضرة بتقنية تردد الراديو

احمد ابراهيم على¹ و احمد عبد المعز عبد الرحمن³

¹قسم العلوم الأساسية ، كلية التربية الصناعية ، جامعة حلوان ، كوبرى القبة ، القاهرة ، مصر .

²مركز بحوث تكنولوجيا النانو ، الجامعة البريطانية في مصر ، مدينة الشروق ، طريق السويس الصحراوي ، القاهرة 11837 .

³معمل إلكترونيات الجوامد ، قسم فيزيقا الجوامد ، شعبة البحوث الفيزيائية، المركز القومي للبحوث ، 33 شارع البحوث ، الدقي ، الجيزة 12622، مصر .

تمت دراسة الاغشية الرقيقة من اكسيد الزنك المحضرة باستخدام تقنية تردد الراديو عند درجات حرارة مختلفة لقاعدة الترسيب تمت دراستها باستخدام الطرق الضوئية.

وتم تحديد كلا من الرتبة الاولى ($\chi^{(1)}$) من القابلية الضوئية الخطية و الرتبة الثالثة من القابلية الضوئية غير الخطية ($\chi^{(3)}$). وكذلك تم دراسة وتحديد معاملات اخري مهمة من النتائج الضوئية غير الخطية مثل معامل الانكسار الغير خطي (n_2) ومعامل الامتصاص غير الخطى (β). وتم ذلك تعيين وحساب القابلية الكهربائية (χ_e) و السماحية النسبية ϵ_p ضوئيا لهذه العينات المحضرة عند درجات حرارة مختلفة لقاعدة الترسيب.

واخيرا تم تعيين وتحديد معاملات ونواتج شبه الموصلة مثل كثافة مستوى طاقة التكافؤ (N_v)، كثافة مستوى طاقة التوصيل (N_c) و تركيز حوامل الشحنات ($N_d - N_a$)، وكذلك تحديد موضع مستوى فيرمي (E_f) وشدة المجال الكهربى عند سطح العينات (E_s) لتلك العينات المحضرة عند درجات حرارة مختلفة لقاعدة الترسيب.